JOURNAL OF MATERIALS SCIENCE **36** (2001) 2359–2367

Impact behavior of aramid fiber/glass fiber hybrid composite: Evaluation of four-layer hybrid composites

ROHCHOON PARK, JYONGSIK JANG*
School of Chemical Engineering, Seoul National University, San 56-1, Shinlimdong Kwanakgu, Seoul, Korea
E-mail: jsjang@plaza.snu.ac.kr

Aramid fiber/glass fiber hybrid composites were fabricated to investigate the impact behavior of four-layer composites through the analysis of delamination area. The effect of position and content of aramid layer on the impact properties of hybrid composites was examined by using driven dart impact tester. The surface-treated composites were prepared by treating the surface of aramid fiber with oxygen plasma and silane coupling agent. The trend of total impact energy was correlated to that of delamination area in both untreated and treated composites. The impact energy and delamination area of hybrid composites depended on the position of aramid layer. When aramid layer was at back surface, the composite exhibited the higher impact energy and delamination area. In surface-treated composites, however, the position of aramid layer had a minor effect on the impact energy of hybrid composites. This was due to the restriction in deformation of aramid fiber. The impact behavior of four-layer hybrid composites was affected by the delamination area at each interface. The deformation at neighbored-aramid layers increased the deformation at adjacent interfaces.

1. Introduction

Aramid fiber/glass fiber hybrid composites can combine advantages of both fibers. The glass fiber provides the high stiffness, high strength, and load-bearing capability, whereas aramid fiber makes the composite more damage tolerant and impact resistant [1–5].

The impact behavior of hybrid composites depends on a great number of design parameters such as laminate thickness, surface treatment, and stacking sequence. It was experimentally found that the energy absorption and damage extent of hybrid composites depended on the laminate thickness [6, 7]. Considering the effect of damage size, it appears that thick laminates are less susceptible to impact damage than thin laminates. Moreover, it has been reported that stacking sequence of hybrid composites plays a major role in determining the impact behaviors of the composites. The position of each layer changed the impact energy and energy absorption mode of hybrid composites [8]. Considering the effect of stacking sequence on the impact properties of hybrid composites, the laminate exhibits the different impact behavior depending on the laminate thickness. The laminate thickness affects the locus of failure, stress distribution, and failure mechanism of composites. Therefore, it is necessary to examine the effect of stacking sequence on the impact behavior of the composites in thin and thick laminate.

The impact energy of aramid fiber-reinforced composites is mainly absorbed by the delamination at interface between laminas [9–11]. Therefore, the impact energy of hybrid composites is closely related to the change of delamination area. However, the relationship between impact behavior and delamination area of hybrid composites has not been well understood with respect to the stacking sequence of the laminate.

In this study, aramid fiber/glass fiber hybrid composites are fabricated to investigate the impact behavior of four-layer composites. The effect of position and surface treatment of aramid layer on impact properties of hybrid composites is studied by using driven dart impact tester. The delamination area of hybrid composites is examined using penetrant injection and deplying technique. In addition, the relationship between impact behavior and delamination area of the hybrid composites is also investigated.

2. Experimentals

2.1. Materials

The aramid fabric used in this study was Kevlar-29 plain weave type from E.I. du Pont de Nemours in the form of a 4800 denier and 480 filament yarn. The S2-glass plain fabric was supplied from Hankook Fiber Co. (Korea) in the form of a 3000 denier and 300 filament yarn. Matrix

* Author to whom correspondence should be addressed.

TABLE I Physical properties of aramid fiber, glass fiber, and vinylester resin

Physical properties	Aramid fiber	Glass fiber	Vinylester resin
Density (g/cm^3)	1.44	2.48	1.15
Tensile modulus (GPa)	62.00	85.50	3.71
Tensile strength (MPa)	2760	4585	63
Elongation to break (%)	3.60	5.40	6.30

resin was styrene-based XSR-10 vinylester resin supplied by National Synthesis Co. (Korea). This resin was modified with a carboxyl-terminated butadiene acrylonitrile (CTBN) rubber for improvement of impact property. The styrene contained in the vinylester resin was used as a crosslinking agent, and dibenzoyl peroxide (BPO) was used as an initiator. The physical properties of aramid fiber, glass fiber, and vinylester resin are given in Table I.

2.2. Fiber surface treatment

The surface of aramid fiber was treated with surface modifiers to investigate the effect of improved adhesion of aramid fiber on impact behavior of hybrid composites. The oxygen plasma treatment and silane coupling agent were used to modify the chemical functionality of aramid fabrics. The plasma output power was 100 W and the flow rate of carrier gas was 10 cc/min. The plasma treatment time was fixed at 1 min. The plasma-treated fabrics were treated with silane coupling agent. γ-methacryloxypropyltrimethoxysilane (γ-MPS) from Petrach System was used as a silane coupling agent for surface treatment. γ-MPS were prehydrolysed for l hr in distilled water adjusted to pH 3.5 with acetic acid. The silane concentration was fixed at 0.3 wt% and the plasma-treated fabrics were impregnated in the prehydrolysed silane solution for 10 min. The silane-treated fabrics were dried for 2 days at room temperature in a hood.

2.3. Prepreg preparation

The vinylester resin, BPO, and acetone were mixed in the weight ratio of 100 : 2 : 10. Acetone was used as a solvent for the BPO and viscosity-reducer of vinylester resin. Each fabric was well impregnated into this mixed solution by hand roller. The resin-impregnated fabrics were aged for 2 days at room temperature in a drying hood for thickening of the mixed resin.

2.4. Composite manufacturing

The composites were made using open leaky mold method in which the pressure is loaded up and down, and the excess resins flow-out both sides. All composites were then cured in a hot press for 20 min at 43 °C and 50 min at 90 °C at a pressure of 7 MPa (1000 psi). The polytetrafluoroethylene film was inserted in the edge of the specimen for easy separation to individual plies after impact. The total volume fraction of fiber in all composites was about 60%. Four-layer hybrid composites were prepared to examine the effect of stacking sequence and surface treatment on the impact properties. Various hybrid configurations were prepared by interleaving plies of aramid and glass fabric. **A** and **G** designated aramid fabric and glass fabric, respectively. The hybrid composite, which consists of three surface layers of aramid and a bottom layer of glass, was designated as **A3G**.

2.5. Impact test

The impact tests were conducted using a Radmana ITR-2000 driven dart impact tester. The composite was clamped horizontally between two plates with an inner diameter of 7.5 cm. The impact tip was hemispherical type with the size of 1.76 cm. The pressure of nitrogen gas was varied to give a range of incident energy and velocity. The impact velocity was fixed at 4.0 m/sec and the incident impact energy was 160 J. Load-displacement curve was recorded and initiation energy, propagation energy, and total energy were calculated. The total impact energy was defined as the sum of the energy absorbed until the maximum load (initiation energy) and the energy absorbed after the maximum load (propagation energy). The dimension of the test specimens was 10 cm $\times$ 10 cm. The impact energies of each specimen were averaged with 5 values.

2.6. Photographs

The damage of hybrid composites after impact was analyzed using manual camera. Both impacted surface and back surface of hybrid composites were observed to examine the relationship between the damaged shape and the absorbed impact energy.

2.7. Delamination area calculation

After impact test, the delamination area of the composites was calculated for the correlation to impact energy. The delamination area of each layer was determined by process of penetrant injection and de-plying. The stamp ink as a penetrant was used to enhance the identification of delaminated areas. The deformed region of composite was easily seen due to red color of stamp ink. The penetrants used prior to de-plying were left in all parts of the damage of composite. After penetrant injection, the composite was separated into individual plies. The delamination area of each ply was measured by tracing the damage area onto poly(ethylene terephthalate)(PET) film and manually measuring the weight of film.

2.8. Scanning electron microscopy (SEM)

The fracture surface of hybrid composites after impact was observed using scanning electron microscopy (SEM). The instrument used in this experiment was Jeol JSM-35, and all specimens were coated with a thin layer of gold to eliminate charging effects.

3. Results and discussion

3.1. Impact property

Table II summarizes impact properties of aramid fiber/glass fiber hybrid composites. Aramid fiber-reinforced composite exhibits higher total impact energy than

TABLE II Maximum load and impact energies of aramid fiber/glass fiber hybrid composites: Untreated aramid fiber

	Maximum load (N)	Initiation energy (J)	Propagation energy (J)	Total energy (J)
G4	4926	9.31	10.33	19.64
AG3	5633	11.50	11.86	23.36
G3A	5044	9.19	12.12	21.31
A2G2	5501	15.26	11.46	26.72
G2A2	6179	17.66	15.66	33.32
AG2A	5646	18.23	10.91	29.14
GA2G	6926	13.83	14.10	27.93
A3G	7763	38.37	16.14	54.51
GA3	8085	44.96	41.80	86.76
A4	7906	51.58	59.15	110.73

TABLE III Maximum load and impact energies of aramid fiber/glass fiber hybrid composites: Surface-treated aramid fiber

	Maximum load (N)	Initiation energy (J)	Propagation energy (J)	Total energy (J)
AG3	6244	11.86	6.32	18.18
G3A	6282	11.65	7.45	19.10
A2G2	6017	11.85	6.67	18.52
G2A2	6395	10.71	9.56	20.27
AG2A	6224	11.20	7.70	18.90
GA2G	7593	15.69	8.22	23.91
A3G	7670	26.89	8.76	35.65
GA3	8689	24.30	14.85	39.15
A4	9178	47.70	33.42	81.12

glass fiber-reinforced composite. The position and volume fraction of aramid layer change the impact property of hybrid composites. When aramid layer is at back surface, the composite exhibits higher total impact energy due to the increase of propagation energy. This means that the degree of deformation at back surface is a major factor to determine the absorption mechanism of impact energy.

The difference in impact energy between composite G4 and A4 is confirmed by the examination of fracture damage after impact. The fracture surfaces of composite G4 and A4 after impact are shown in Fig. 1. Both photographs show the back surfaces of the composites. The stiff composite G4 leads to the localized deformation contrasted with white color (Fig. 1a). This is caused by the high stress generated close to the point of impact. The impact stress is not dispersed into wider region of composite due to the brittle property of glass fiber, and the impact energy is absorbed only at a small area of composite. However, the flexible composite A4 exhibits the wider deformation area through the formation of dome (Fig. 1b). The high impact toughness of aramid fiber enables the composite to undergo the full deformation, leading to a considerable degree of plastic deformation.

The impact properties of hybrid composites with surface treatment of aramid fiber are represented in Table III. Compared with Table II, the total impact energy of composite decreases significantly due to the improvement of interfacial adhesion strength between fiber and matrix. Unlike the case of untreated composites, the position of aramid layer has a minor effect on total impact energy of hybrid composites. Although aramid layer is at back surface, the composite exhibits the low impact energy because the improved adhesion of composites restricts the deformation of aramid layer. As a result, the restraint of deformation at back surface also plays a role in controlling the impact properties of hybrid composites.

The impact properties of thick composites are primarily dominated by local stress rather than plate bending stress [7]. This means that the impact properties of four-layer hybrid composites depend on the position of aramid layer. Fig. 2 shows the total impact energy of hybrid composites with aramid layer at back surface as a function of aramid fiber content. As the volume fraction of aramid fiber increases, the total impact energy of

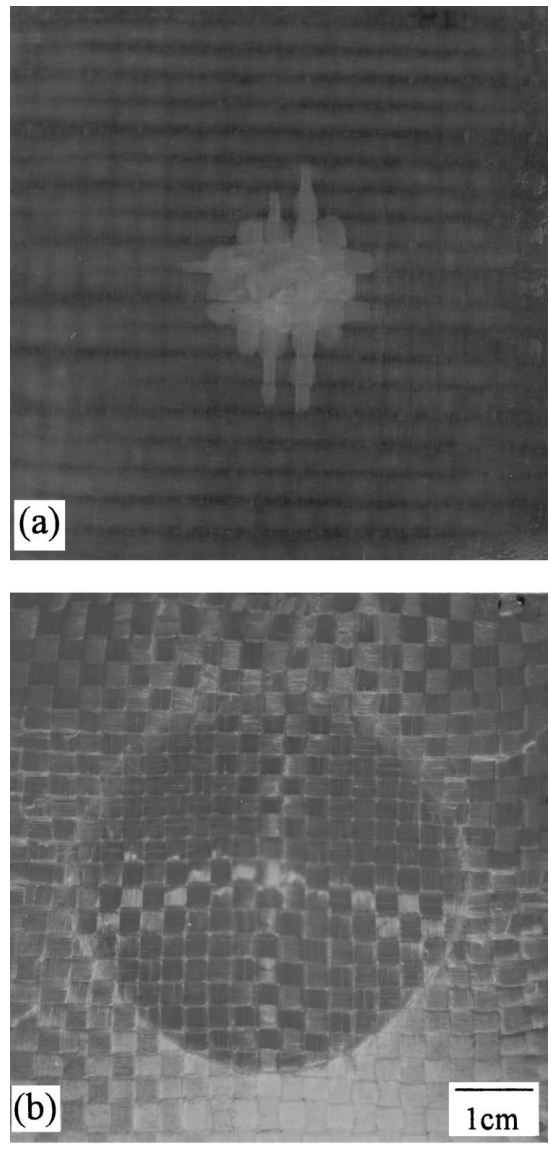

Figure 1 The fracture surfaces of composite G4 and A4 after impact: (a) back surface of composite G4, (b) back surface of composite A4.

composites increases. The increase of impact energy is very large at volume fraction of 75%. In thick composites, the impact damage initiates on the impacted surface by the large local stress generated close to the point of impact [7]. This indicates that the layer at impacted surface cannot undergo the full deformation because adjacent layers restrict its deformation. The layers at back surface experience a much amount of deformation

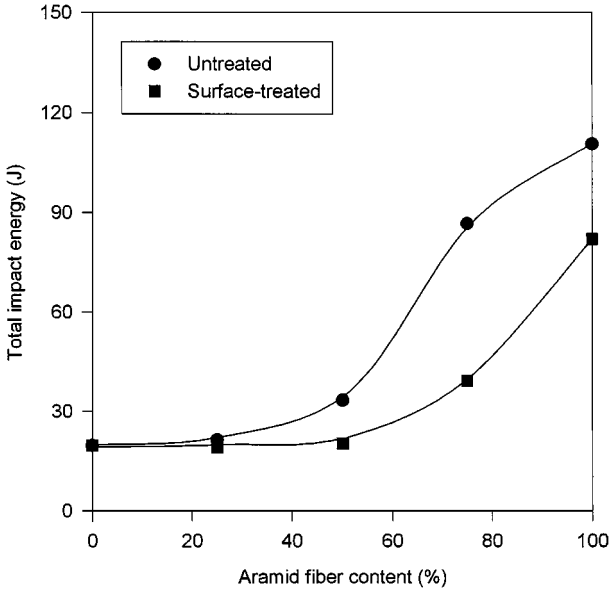

Figure 2 The total impact energy of hybrid composites with aramid layer at back surface as a function of aramid fiber content.

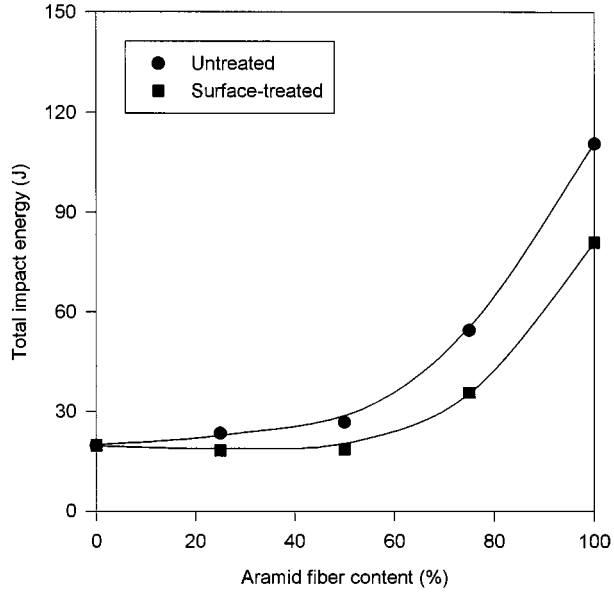

Figure 4 The total impact energy of hybrid composites with aramid layer at impacted surface as a function of aramid fiber content.

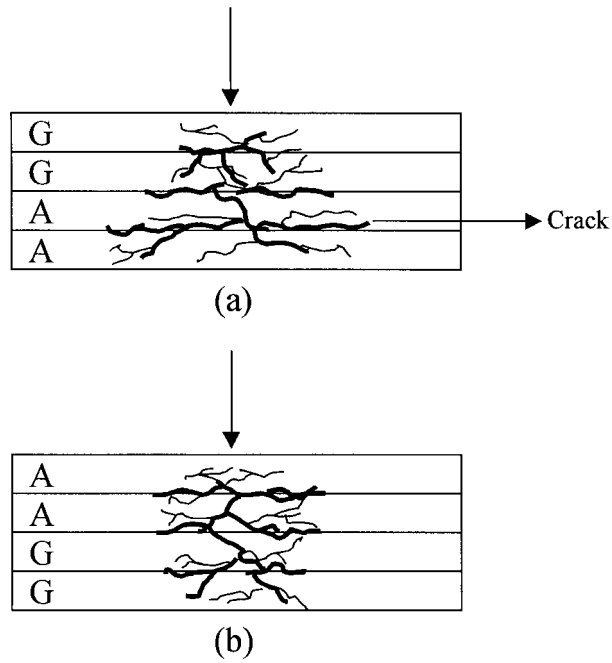

Figure 3 The impact damage of (a) composite G2A2 and (b) composite A2G2.

after the initial failure. The degree of deformation increases as the impact propagates from impacted surface to back surface. Therefore, when aramid layer is at back surface, the composite absorbs much impact energy through large deformation of aramid layers (Fig. 3a). On the other hand, the surface treatment of aramid fiber decreases the impact energy of composites. Especially, the decrement is large at volume fraction of 75%. This is attributed to the fact that the surface treatment of aramid fiber enlarges the brittleness of composite, and restricts the deformation of aramid layer at back surface. The hydroxyl group of γ-MPS forms chemical bonding with hydroxyl group of aramid fiber, and the double bond makes it possible to induce the chemical bonding with vinylester matrix during the curing process. The strong bonding at the fiber/matrix interface tends to restrain delamination and fiber pull-out, leading to a small deformation area. From these results, it is concluded that the impact energy is primarily dissipated through plastic deformation of ductile aramid layer at back surface.

Fig. 4 shows the total impact energy of hybrid composites with aramid layer at impacted surface as a function of aramid fiber content. The total impact energy increases with increasing volume fraction of aramid fiber. However, the increase of impact energy is not large compared with Fig. 2. Aramid layer at impacted surface cannot experience the full deformation because the adjacent layers restrict its deformation. Moreover, the stiff glass layer at back surface has the tendency to inhibit aramid layers from flexing and deforming plastically during impact (Fig. 3b). The surface treatment of aramid fiber reduces the total impact energy of composites, but the decrement is small compared with Fig. 2. This is caused by the fact that aramid layer at impacted surface does not play a major role in absorbing the impact energy.

The fracture surfaces at region near impact point of composite G2A2 and A2G2 are compared in Fig. 5. In composite G2A2 (Fig. 5a), it can be seen that the distance between glass and aramid fiber is very large. This indicates that aramid fibers at back surface are fully deformed after initial failure of glass fiber. In case of composite A2G2 (Fig. 5b), aramid and glass fiber fail simultaneously and the deformation of aramid fibers is restricted by glass fibers at back surface.

The difference in impact energy of hybrid composites can be reflected by the change of load-displacement curves. Fig. 6 shows load-displacement curves of composite GA3 and A3G. The impact response of untreated composites appears to be dominated by the large displacement. In composite GA3, the load drops gradually and stepwise after maximum load, indicating that the impact energy is absorbed up to larger displacement due to extensive deformation at aramid layers or at aramid-aramid layer interface. The composite A3G

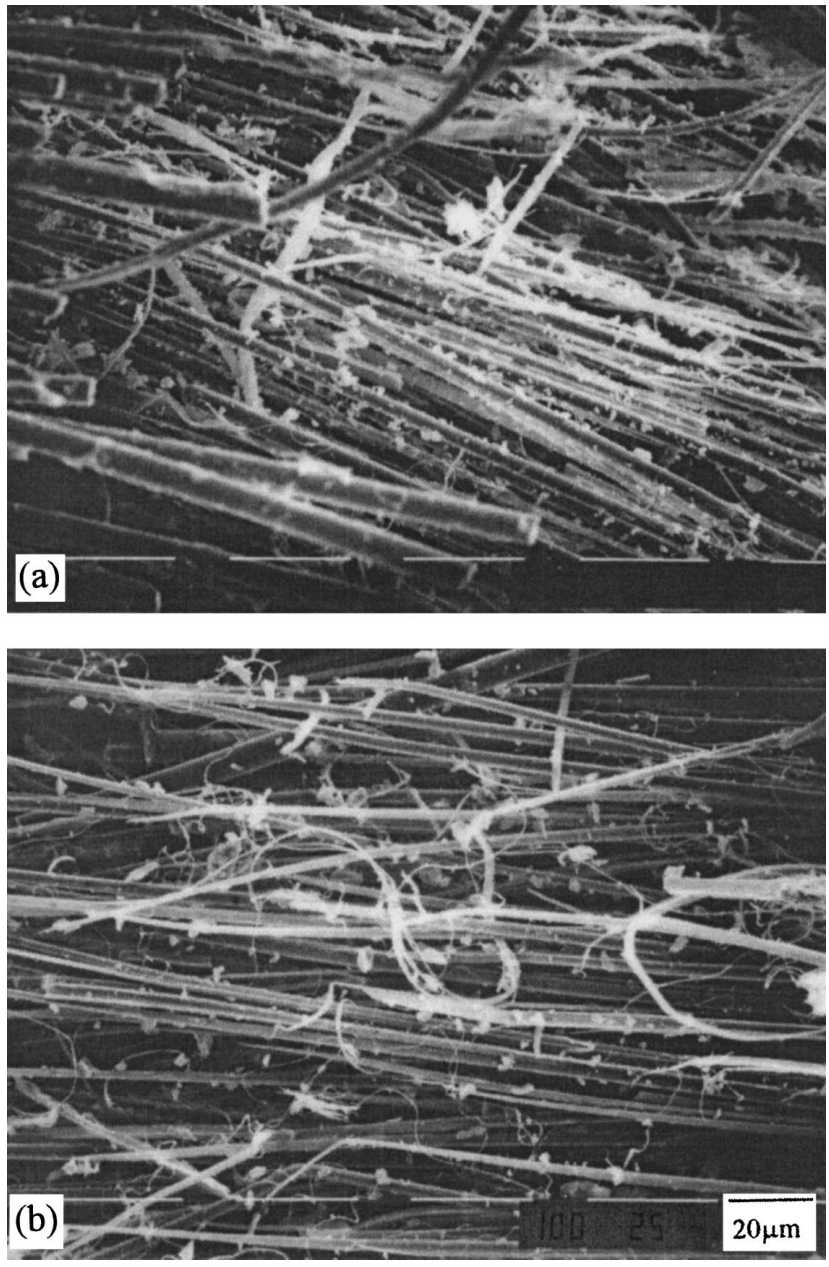

Figure 5 The fracture surfaces at region near impact point of (a) composite G2A2 and (b) composite A2G2.

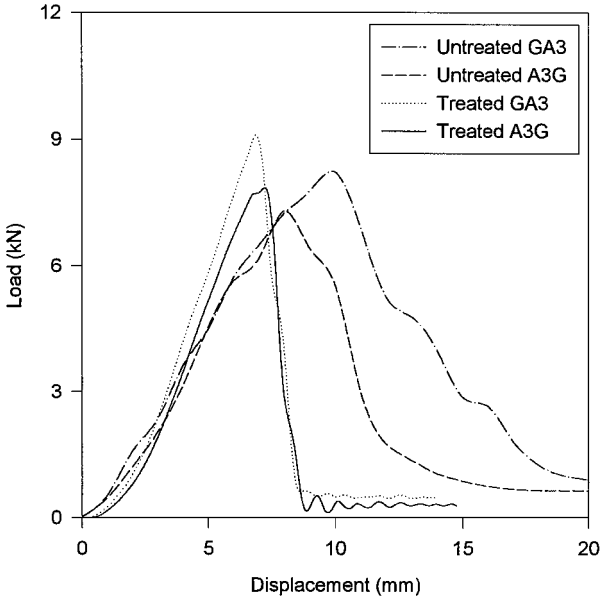

Figure 6 The load-displacement curves of composite GA3 and A3G.

shows rather rapid load-drop after maximum load because glass layer at back surface restrains the deformation of aramid layers at impacted surface. The surface-treated composites exhibit the lower displacement at break compared with untreated composites. Furthermore, the surface treatment of aramid layer increases the initial slope of load-displacement curve and the load drops rapidly after maximum load. This is caused by the restriction in deformation due to improved interfacial strength of composite. As a result, the surface-treated composites exhibit the low total impact energy due to the large decrease of displacement at break.

3.2. Delamination area

The impact energy of aramid fiber-reinforced composites is mainly absorbed by the fiber-matrix debonding and the delamination at interface between laminas [9–11]. Especially, in laminated structure, the delamination plays a major role in absorbing the impact

TABLE IV Delamination area of aramid fiber/glass fiber hybrid composites with aramid layer at back surface

		Delamination area (cm^2)			
		Untreated		Surface-treated	
	G/G1	8.61		-	
G4	G/G2	8.61	25.83	-	-
	G/G3	8.61		-	
	G/G1	5.89		4.71	
G3A	G/G2	13.17	44.96	10.46	38.94
	G/A3	25.90		23.77	
	G/G1	16.93		9.93	
G2A2	G/A2	43.58	124.23	28.62	80.35
	A/A3	63.72		41.80	
	G/A1	52.83		26.57	
GA3	A/A2	59.38	171.74	40.18	106.71
	A/A3	59.53		39.96	
	A/A1	8.39		25.62	
A4	A/A2	21.49	76.38	25.92	74.81
	A/A3	46.50		23.27	

TABLE V Delamination area of aramid fiber/glass fiber hybrid composites with aramid layer at impacted surface

		Delamination area (cm^2)			
		Untreated		Surface-treated	
	G/G1	8.61		-	
G4	G/G2	8.61	25.83	-	-
	G/G3	8.61		-	
	A/G1	23.18		23.62	
AG3	G/G2	11.55	41.13	10.05	38.45
	G/G3	6.40		4.78	
	A/A1	37.75		36.72	
A2G2	A/G2	32.97	86.98	23.77	71.10
	G/G3	16.26		10.61	
	A/A1	50.92		34.37	
A3G	A/A2	51.07	140.17	33.93	92.21
	A/G3	38.18		23.91	
	A/A1	8.39		25.62	
A4	A/A2	21.49	76.38	25.92	74.81
	A/A3	46.50		23.27	

energy. Therefore, the delamination area of composites is a dominant factor to evaluate impact properties of hybrid composites. The delamination area of four-layer hybrid composites with aramid layer at back surface is shown in Table IV. The delamination area was calculated at three interface regions and the total delamination area was defined as the sum of three delamination areas. G/G1 means the interface between the first glass layer and the second glass layer from impacted surface, and G/A3 means the interface between the third glass layer and the fourth aramid layer. The trend of total delamination area is similar to that of total impact energy in both untreated and treated composites. However, composite A4 exhibits lower delamination area than composite GA3. This can be explained from the fact that the impact energy is related to the indentation depth as well as the delamination area. In load-displacement curve, the displacement at break is related to indentation depth of composites. In spite of low delamination area, composite A4 shows the highest impact energy due to the large displacement at break (Fig. 7). On the other hand, the delamination area at each interface exhibits the different values due to local stress of hybrid composites. The delamination area of back surface is larger than that of front surface. This is due to easy deformation of aramid layers at back surface.

The delamination area of hybrid composites with aramid layer at impacted surface is shown in Table V. The total delamination area of untreated and treated composites is small compared with Table IV. This is consistent with the result of total impact energy. In the surface-treated composites, the decrement of delamination area is not large because aramid layers at front surface suffer the restricted deformation even in untreated composites.

The position of aramid layer changes the impact energy and delamination area of hybrid composites. Furthermore, the delamination area at each interface exhibits the different results depending on the stacking sequence of the composites. This indicates that the delamination area at each interface has an important effect on the impact behavior of hybrid composites. The

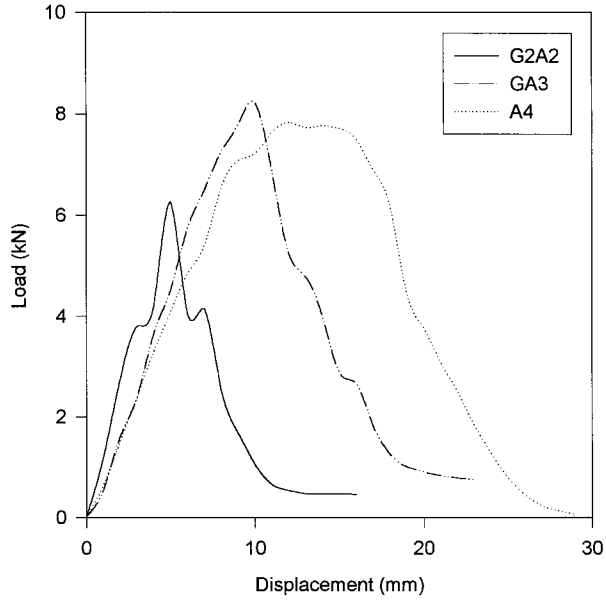

Figure 7 The load-displacement curves of composite G2A2, GA3, and A4.

change of delamination area at interface G/A is shown in Fig. 8. When aramid or glass layer is added to composite GA, delamination area at interface G/A changes according to the position of added layer. The composite G2A2 and GA3 exhibit the larger delamination area at interface G/A. This is due to the presence of aramid layers adjacent to component GA. The large deformation at interface A/A leads to additional deformation at interface G/A. This result can be confirmed by reducing the deformation at interface A/A. The delamination area of composite G2A2 and GA3 decreases remarkably by surface treatment of aramid layer. The other evidence of above result is that the delamination area of composite GA2G is lower than that of composite GA3. From these results, it is concluded that the neighbored aramid layers play a role in increasing the deformation at other interface.

The effect of added layer on additional deformation at interface G/A is compared in Fig. 9. The red-colored region is observed by the diffusion of a penetrant through

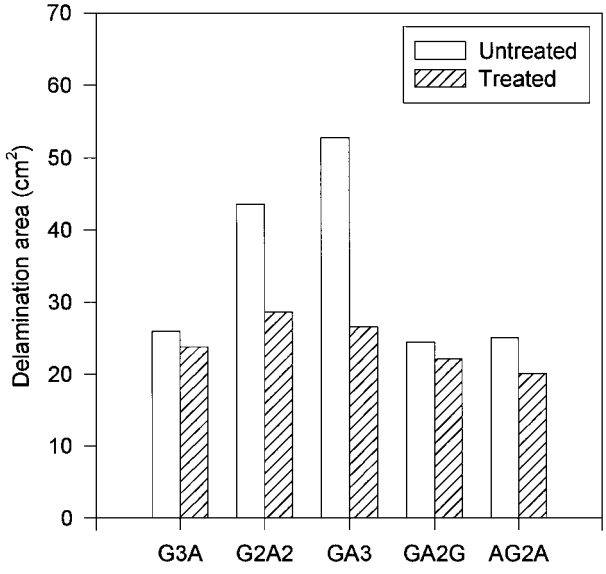

Figure 8 The change of delamination area at interface G/A according to the position of added layer.

delaminated region between laminas. The delamination area at interface G/A is larger in composite GA3 (Fig. 9a) than in composite GA2G (Fig. 9c). Fig. 9a shows wider red-colored region due to additional deformation, whereas Fig. 9c shows the narrow red-colored region due to restricted deformation. Furthermore, the surface treatment of aramid layer leads to the narrow red-colored region compared with untreated composite (Fig. 9b).

Fig. 10 exhibits the effect of layer addition on delamination area at interface A/G. The delamination area is larger in composite A2G2 and A3G than in other composites. As shown in Fig. 8, the deformation at interface A/A plays a role in increasing the deformation at interface A/G. This result can be explained by restraining the deformation at interface A/A. The delamination area of surface-treated composites is very low, and this indicates that restriction of deformation at interface A/A does not induce the additional deformation at interface A/G. The reduced red-colored region of surface-treated

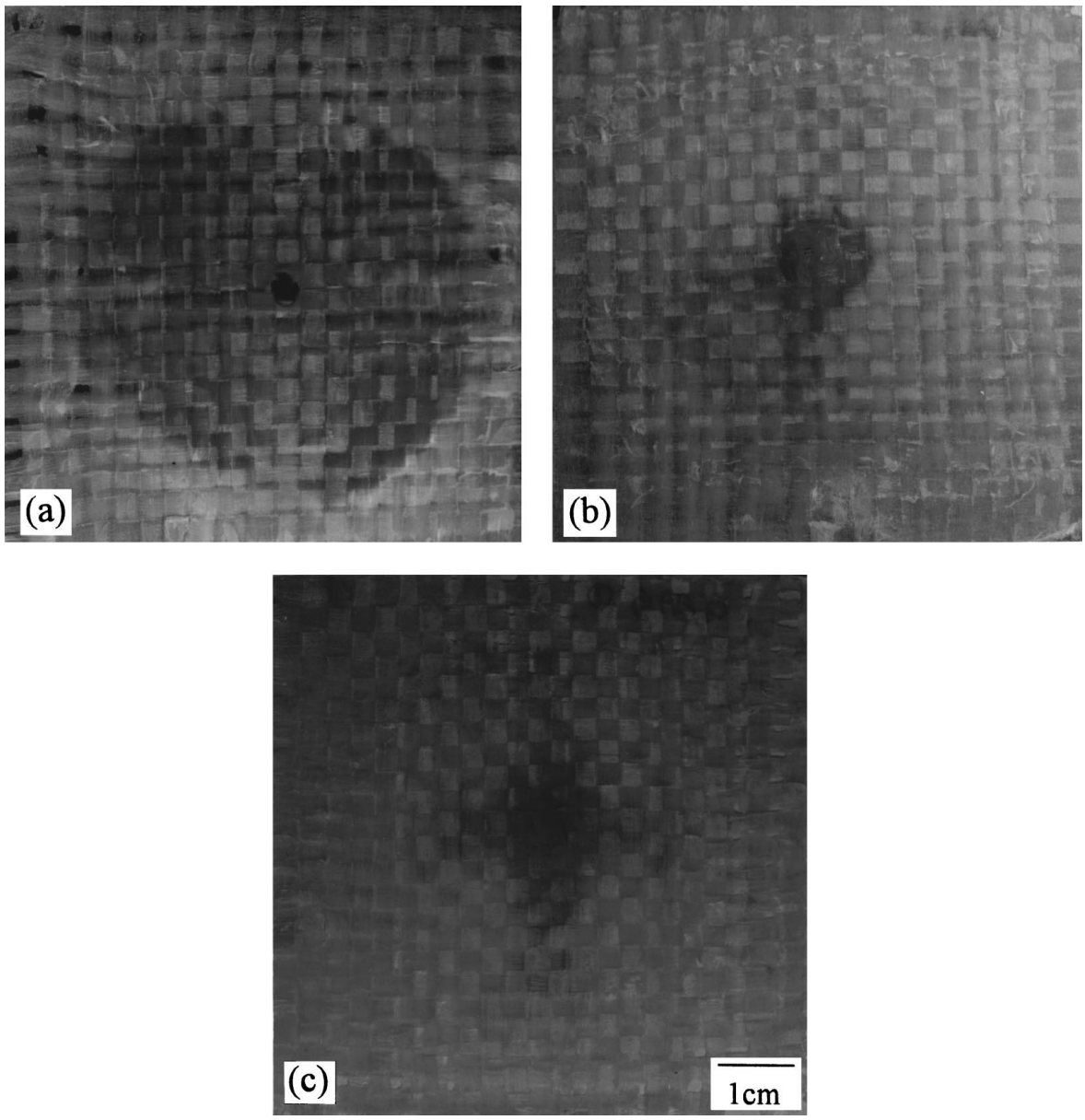

Figure 9 Photographs showing delamination area at interface G/A: (a) untreated composite GA3, (b) surface-treated composite GA3, (c) untreated composite GA2G.

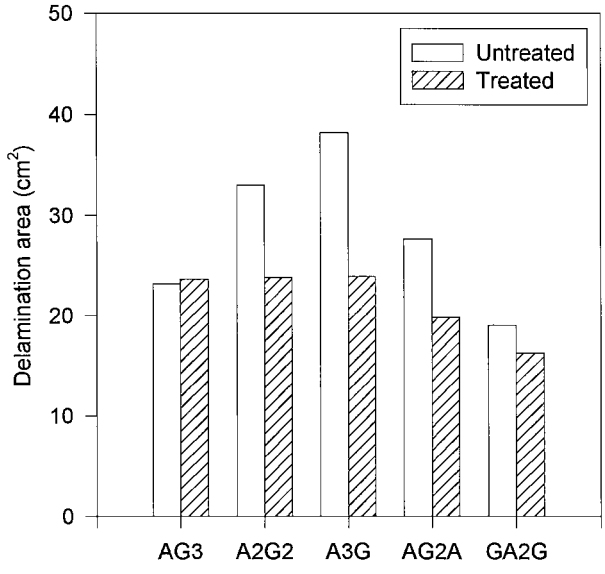

Figure 10 The effect of layer-addition on delamination area at interface A/G.

composite A3G is shown in Fig. 11b. Furthermore, composite GA2G exhibits much lower delamination area than composite A3G. This is caused by the fact that composite GA2G does not contain the component leading to additional deformation at interface A/G. The damage zone at interface A/G is larger in composite A3G (Fig. 11a) than in composite GA2G (Fig. 11c).

The comparison of delamination area at interface G/G is shown in Fig. 12. When the component AA is at front surface or back surface of component GG, the aramid layers affect the deformation at interface G/G. The composite A2G2 and G2A2 exhibit the large delamination area due to the additional deformation at interface G/G by adjacent aramid layers. The surface treatment of aramid layer decreases the delamination area of composite A2G2 and G2A2. This indicates that the deformation at interface G/G is affected by the deformation of aramid layers.

The delamination area at interface A/A of each composite is shown in Fig. 13. Although the total impact

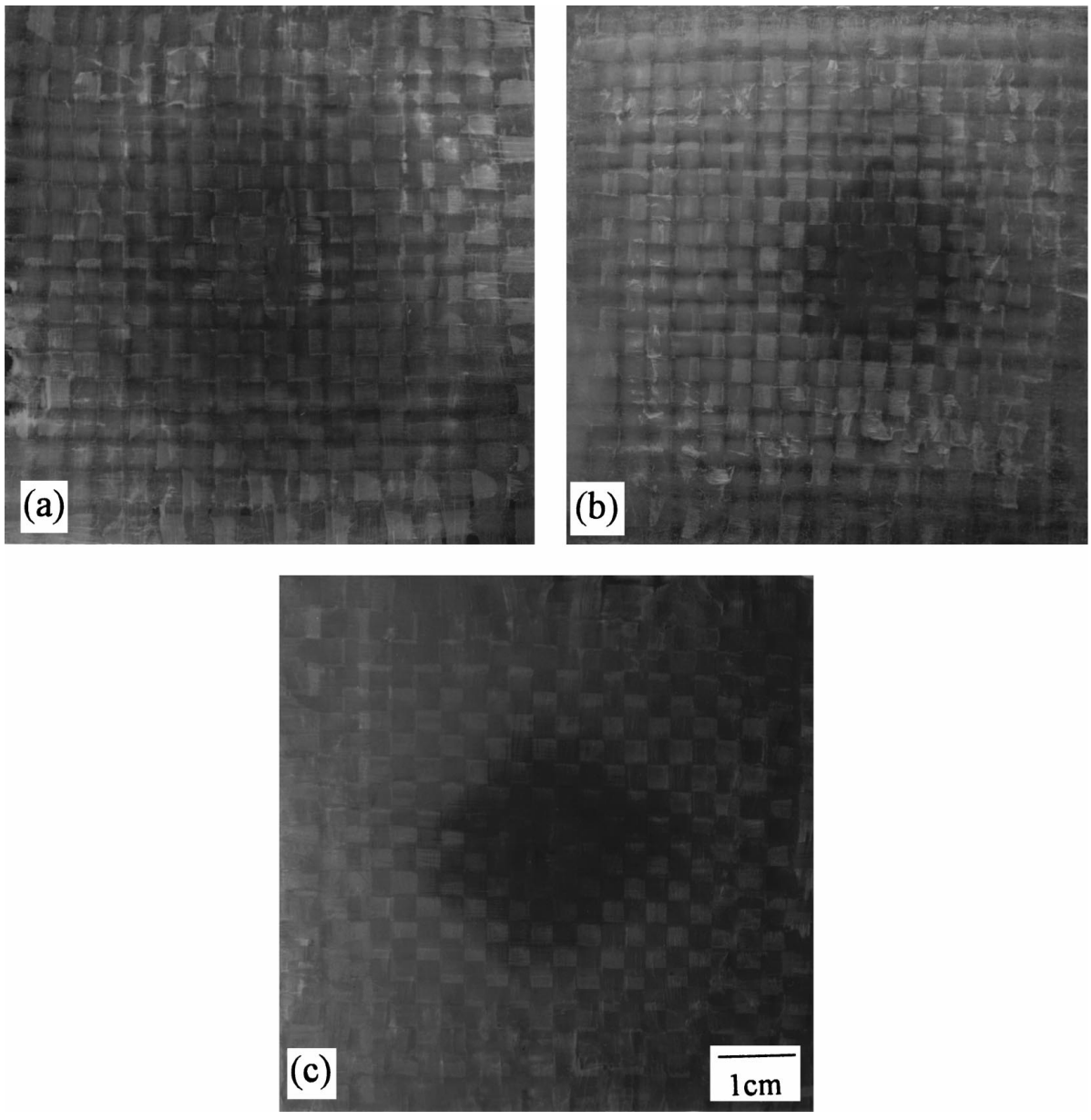

Figure 11 Photographs showing delamination area at interface A/G: (a) untreated composite A3G, (b) surface-treated composite A3G, (c) untreated composite GA2G.

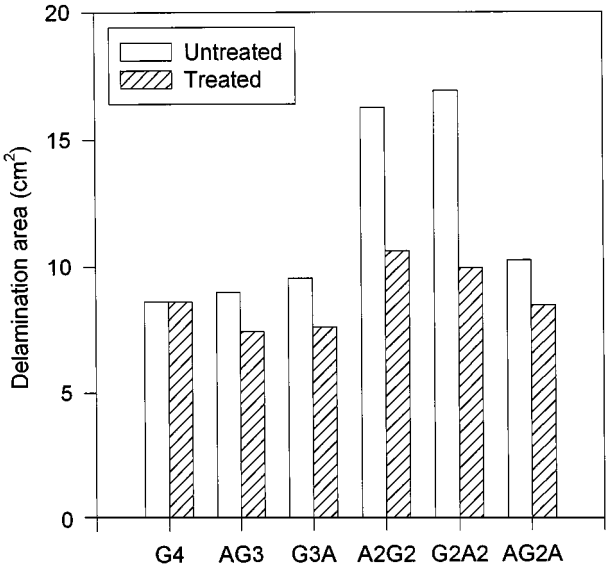

Figure 12 The change of delamination area at interface G/G according to the position of added layer.

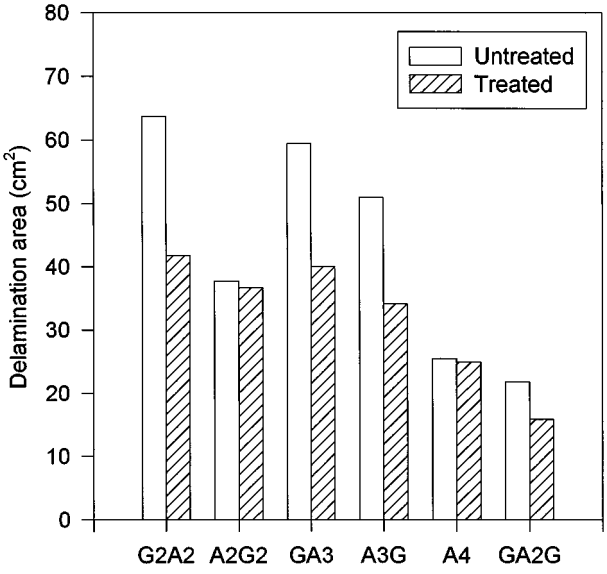

Figure 13 The change of delamination area at interface A/A according to the position of added layer.

energy of composite A4 is largest, the composite exhibits the smaller delamination area. The delamination area of composite A4 was averaged with values at three interface A/A. As shown in Table IV, the composite shows the large difference of delamination area at each interface. The impact energy of composite A4 is primarily affected by the displacement at break rather than the delamination area as shown in Fig. 7.

4. Conclusions

The impact behavior of four-layer aramid fiber/glass fiber hybrid composites was investigated through the analysis of delamination area. The trend of impact properties was well correlated to that of delamination area in both untreated and treated composites. The impact damage initiated on the impacted surface by the large local stress generated close to the point of impact. When aramid layer was at back surface, the composite exhibited the higher impact energy and delamination area. The impact energy was primarily dissipated through plastic deformation of aramid layers at back surface, whereas the aramid layer at impacted surface did not undergo the full deformation because adjacent layers restricted its deformation. In surface-treated composites, the position of aramid layer had a minor effect on the total impact energy of hybrid composites. This was due to the restriction in deformation of aramid fiber. The composite A4 exhibited the highest impact energy in spite of low delamination area. This was attributed to the fact that the impact energy was related to the indentation depth as well as the delamination area. The delamination area at each interface had an important effect on the impact behavior of hybrid composites. The deformation at neighbored-aramid layers increased the deformation at adjacent interfaces, and much impact energy was dispersed at the interface through the enhanced deformation.

Acknowledgment

This research has been carried out by Research Institute of Engineering Science (RIES) and the authors gratefully acknowledge the research support of RIES. This work was also supported by a grant No. KOSEF 95-0300-02-04-3 from the Korea Science and Engineering Foundation.

References

1. J. KALANTAR and L. T. DRZAL, *J. Mater. Sci.* **25** (1990) 4194.
2. *Idem., ibid.* **25** (1990) 4186.
3. J. R. BROWN, P. J. C. CHAPPELL and Z. MATHYS, *ibid.* **26** (1991) 4172.
4. J. R. BROWN and Z. MATHYS, *ibid.* **32** (1997) 2599.
5. G. S. SHEN and S. S. SHYU, *Compos. Sci. Technol.* **52** (1994) 489.
6. D. STAVROPOULOS and G. C. PAPANICOLAOU, *J. Mater. Sci.* **32** (1997) 931.
7. J. A. ZUKAS, T. NICHOLAS, H. F. SWIFT, L. B. GRESZCZUK and D. R. CURRAN, "Impact Dynamics" (John Wiley & Sons, New York, 1982) p. 55.
8. A. A. J. M. PEIJS, R. W. VENDERBOSCH and P. J. LEMSTRA, *Composites* **21** (1990) 522.
9. S. BAZHENOV, *J. Mater. Sci.* **32** (1997) 4167.
10. B. Z. JANG, L. C. CHEN, C. Z. WANG, H. T. LIN and R. H. ZEE, *Compos. Sci. Technol.* **34** (1989) 305.
11. Y. W. MAI and F. CASTINO, *J. Mater. Sci.* **19** (1984) 1638.

Received 24 August 1999
and accepted 26 September 2000